

Schottky barrier height modulation by atomic dipoles at the silicide/silicon interface

Yoshifumi Nishi, Takashi Yamauchi, Takao Marukame, Atsuhiko Kinoshita, Junji Koga, and Koichi Kato
*Advanced LSI Technology Laboratory, Corporate Research and Development Center, Toshiba Corporation,
 8, Shinsugita-Cho, Isogo-Ku, Yokohama 235-8522, Japan*

(Received 6 October 2010; revised manuscript received 13 August 2011; published 26 September 2011)

We studied the behavior of boron (B) atoms around the nickel silicide (NiSi)/silicon (Si) interface through first-principles calculations. We found that B atoms, absorbed at the most stable substitutional sites on the Si side along the interface, dramatically reduce the Schottky barrier height (SBH) for a hole owing to atomic-scale electric dipoles generated between the ionized B atom and the induced image charge in the NiSi layer. We also found that this interface dipole generation leads to an increase of several orders of magnitude in the B solubility limit around the interface, enhancing SBH modulation. The possibility of interface atomic dipoles reducing the SBH was verified by both the observed B profiles and the measured I - V characteristics of the B-implanted NiSi/Si Schottky diodes.

DOI: 10.1103/PhysRevB.84.115323

PACS number(s): 73.30.+y, 73.40.Ns

I. INTRODUCTION

The origin of Schottky barrier height (SBH) at the metal-semiconductor interface and the control of SBH have been fundamental issues of semiconductor physics for several decades. Theoretical models based on gap states at the interface¹⁻⁵ were proposed to account for the Fermi-level pinning effect. Among these models metal induced gap state (MIGS) model¹⁻³ has been widely accepted as a basic principle of metal-semiconductor interfaces. The MIGS model makes a definite prediction for the Schottky barrier height whose value depends only on the identity of the materials on the two sides of the interface. An experiment⁶ and first-principles calculation⁷ have shown, however, that the SBH depends on the atomic structure of the interface. This fact indicates that not only bulk-terminated interface states but also the atomic scale electronic structures at the interface are essential to understand the physics of metal-semiconductor interfaces.

Molecular approaches pointed out that polarized chemical bondings across the interface can lead to the Fermi-level pinning effect.^{8,9} Dipoles across the interface induced by charge transfer among atoms at the interface have a substantial contribution to SBH.^{10,11} This means that a drastic change of SBH is possible even for metal-covalent semiconductor interfaces, if impurity atoms doped in the vicinity of the interface can induce dipoles across the interface.

A metal-semiconductor interface with heavily doped impurities in the semiconductor is generally used as an ohmic contact electrode, but atomic scale physics in the interface has not been understood very well. A quantitatively precise approach is essential to study the electronic structure at the interface since the charge polarizations strongly depend on the crystallographic structure and component atoms.

In the present work, we explore the possible impurity-induced dipoles and their effects on the SBH through first-principles calculations and experimental verification. For a model of silicide/Si junction, we employed nickel monosilicide (NiSi) and Si as a metal and a host semiconductor. This is because NiSi is obtained by solid-phase reaction between Si substrate and Ni thin film deposited on the substrate so that NiSi/Si interface is atomically clean.¹² Therefore the NiSi/Si

junction is ideal for studying physics of metal-semiconductor interfaces in atomic scale.

II. THEORETICAL CALCULATIONS

A. Calculation methods

Our calculations are based on density functional theory with generalized gradient approximation (GGA) including spin polarization.¹³ Ultrasoft pseudopotentials¹⁴ are used for the specific atoms with 64- and 16- k points for Brillouin zone samplings in the bulk and the junction structures, respectively. We employed the cutoff energies of 25 Ry for the wave functions and 196 Ry for the augmented electron densities that are sufficient for converging energies.

1. Bulk-dopant formation energies

Formation energies¹⁵ of a B atom at interstitial and substitutional sites were calculated for bulk Si and NiSi as well as NiSi/Si junction structures to discuss the behavior of B atoms in the vicinity of the interface. A unit cell for bulk calculation consists of 64 atoms both for Si and NiSi. The NiSi structure used in this study is the MnP-type orthorhombic one with lattice constants of $a = 5.62$, $b = 3.34$, and $c = 5.18$ Å.^{16,17}

The formation energy of a B atom in the interstice $E_{\text{fm}}(\text{B}^{\text{int}})$ is expressed by

$$E_{\text{fm}}(\text{B}^{\text{int}}) = E(\text{Mat}) + E(\text{B}) - E(\text{Mat} + \text{B}^{\text{int}}), \quad (1)$$

where Mat represents material species NiSi or Si, $E(\text{Mat} + \text{B}^{\text{int}})$ and $E(\text{Mat})$ are the energies of bulk Mat with and without an interstitial B atom, respectively, and $E(\text{B})$ is the energy of a B atom in the vacuum.

Likewise, those at the Si-substitutional site $E_{\text{fm}}(\text{B}^{\text{Si}})$ and at the Ni-substitutional site $E_{\text{fm}}(\text{B}^{\text{Ni}})$ are written by

$$E_{\text{fm}}(\text{B}^{\text{Si}}) = E(\text{Mat}) + E(\text{B}) - E(\text{Mat} + \text{B}^{\text{Si}}) + E(\text{Si})/N_{\text{Si}} - E(\text{NiSi})/N_{\text{Ni}}, \quad (2)$$

$$E_{\text{fm}}(\text{B}^{\text{Ni}}) = E(\text{NiSi}) + E(\text{B}) - E(\text{NiSi} + \text{B}^{\text{Ni}}) + E(\text{Si})/N_{\text{Si}} - E(\text{NiSi})/N_{\text{Ni}}, \quad (3)$$

respectively, where $E(\text{Mat} + \text{B}^{\text{Si}})$, N_{Si} and N_{Ni} are the energy of bulk Mat with a B atom in a Si-substitutional site, the

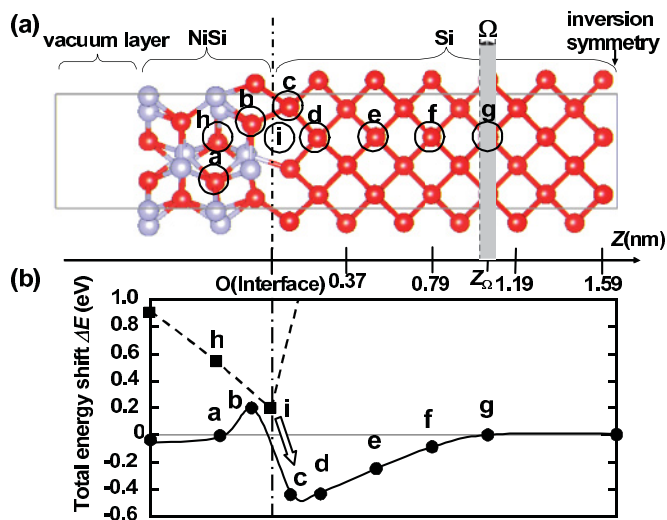


FIG. 1. (Color online) (a) Calculated atomic structure of the NiSi/Si interface. Red and light blue balls stand for Si and Ni atoms, respectively. (b) Total energy shifts (ΔE 's) of the interfacial structure with a B atom placed at a substitutional site [labeled from a to g in (a)] and at interstitial site (h and i) are drawn by solid and broken curves, respectively.

number of Si atoms in the bulk Mat and the number of Ni atoms in the bulk NiSi. Note that $E_{\text{fm}}(\text{B}^{\text{Ni}})$ in Eq. (3) can be defined for NiSi only.

In these calculations, we assume that a Si atom replaced by a B atom moves into the bulk Si to form a Si crystal, which is taken into Eq. (2) as the last term. Similarly, the last two terms are added to Eq. (3) according to our assumption that a Ni atom replaced by a B atom reacts with a Si atom in the bulk Si to form NiSi.

2. LDOS and SBH at the junction

The calculated junction structure comprises a vacuum layer/four NiSi layers/12 Si layers as shown in Fig. 1(a), where the thickness of the vacuum layer is the same as that of three Si layers. NiSi (010)/Si (001) is assumed as the crystallographic orientation at the interface, which is an experimentally confirmed arrangement.^{18–20} Inversion symmetry is imposed at the end of the Si layer for computational efficiency in dealing with the periodic boundary condition.¹⁵ This doubles the number of atoms in the calculated structure; the supercell includes 40×2 and 160×2 atoms for (1×1) and (2×2) unit cell calculations, respectively. All the atoms except the Si atoms at the right-side end were relaxed to be in equilibrium positions.

The unit cell is divided into 50 equal slices Ω identified by Z_Ω , the distance from the NiSi/Si interface as shown in Fig. 1(a). We calculated the local density of states (LDOS) of each slice. The energy difference between the Fermi level and the valence band edge of LDOS on the Si side of the interface gives the SBH, as described in the following section. In this evaluation, quasiparticle correlations for SBH were not included for simplicity.

TABLE I. Calculated formation energies.

	$E_{\text{fm}}(\text{B}^{\text{int}})$ (eV)	$E_{\text{fm}}(\text{B}^{\text{Si}})$ (eV)	$E_{\text{fm}}(\text{B}^{\text{Ni}})$ (eV)
NiSi	4.28	5.24	4.55
Si	2.61	5.19	...
0			

B. Formation energy of a B atom

The calculated formation energies of a B atom at interstitial and substitutional sites in the bulk NiSi and Si are listed in Table I. We found that $E_{\text{fm}}(\text{B}^{\text{Si}})$ is the largest in both NiSi and Si cases, indicating that the Si-substitutional site is the most energetically favorable for a B atom in NiSi as well as Si. Although Ni and B atoms substituted in a bulk Si feel slight repulsion as their atomic distance is reduced, the small B atom is more stable at a Si-substitutional site than at Ni-substitutional site in NiSi because the atomic radius of Si is smaller than Ni. We will assume, therefore, a B atom in NiSi to be at a Si substitutional site in the following discussion.

It should be noted that both formation energies $E_{\text{fm}}(\text{B}^{\text{int}})$ and $E_{\text{fm}}(\text{B}^{\text{Si}})$ for NiSi are larger than those for Si. Hence it seems to be impossible to accomplish a NiSi/Si junction with high B concentration because B atoms would easily diffuse into NiSi from Si. But it is possible, as will be shown below, both theoretically and experimentally.

Figure 1(b) shows the total energy shift (ΔE) of the NiSi/Si junction structure with a B atom as a function of the B position (a horizontal axis of z is defined as the distance from the interface of NiSi/Si). The calculations were performed following the same procedure expressed by the Eqs. (1), (2), and (3). The origin ($\Delta E = 0$) is the energy with a B atom at a substitutional site in Si far from the interface [i.e., $E_{\text{fm}}(\text{B}^{\text{Si}})$ in bulk Si]. Solid and dashed lines correspond to the case of a B at the Si substitutional site and in the interstice, respectively. ΔE 's on the left-side edge of solid and dashed lines (-0.05 and 0.91 eV) are calculated using bulk NiSi structures.

As can be seen in Fig. 1(b), ΔE is the lowest (-0.45 eV) at the position c. We attribute this energetic valley structure to charge transfer among the atoms at the interface. In fact, we calculated the effective charges on the atoms by summing the charge densities within its Wigner-Seitz cell, which can be calculated at grid points generated regularly on Cartesian coordinates.¹⁵ Figure 2 shows the calculated charge

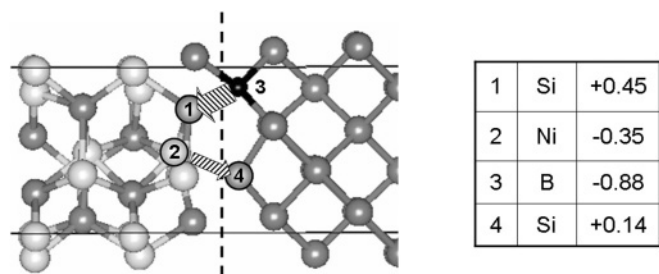


FIG. 2. Electric dipoles at the interface illustrated by the hatched arrows. The calculated effective charges on the atoms from 1 to 4 are shown in the table on the right. The gray and white balls stand for the same as those in Fig. 1(a), and the black ball stands for a B atom.

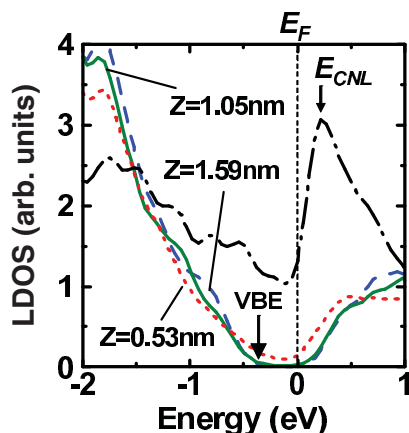


FIG. 3. (Color online) Calculated LDOS in Si near the intrinsic NiSi/Si. Those at the interface, 0.53, 1.05, and 1.59 nm from the interface are plotted by dashed, dotted, solid, and broken lines, respectively.

distribution when a B atom is placed at the position labeled 3 [corresponding to the position c in Fig. 1(a)]. The Si atom on the NiSi side of the interface (labeled 1) is positively charged to $+0.45e$, while the B atom on the Si side is negatively charged to $-0.88e$ (e represents the elementary electric charge). This indicates that the B atom is energetically stabilized by forming an electric dipole with the Si atom on the NiSi side; the local electric field of the dipole lowers the energy of the B atom at the interface. This dipole energy can be estimated as -0.56 eV by the Coulomb energy $E = -Q^{*2}/4\pi\epsilon a$, where Q^* , a , and ϵ are the effective charge of the B atom ($-0.88e$), the distance between the B atom and its image charge (1.66 Å), and the Si dielectric constant, respectively. Although this is a rough estimation, the obtained value is quite close to ΔE .

C. SBH modulation at NiSi and Si interface

As shown in Fig 2, another electric dipole exists between Ni 2 and Si 4, which is an intrinsic dipole across the NiSi (010)/Si (001) interface. The directions of the B-induced and intrinsic dipoles are opposite, but the larger B-induced dipole overcompensates the intrinsic one. We thus expect that this local electric field across the interface induced by B incorporation can modulate the SBH.

Figure 3 shows the calculated LDOS for the NiSi/Si interface without dopants using a (2×2) unit cell. Since the metallic state penetrates into the Si layer, the Si band gap does not fully open in the LDOS until $z = 1.05$ nm. A large peak of LDOS appears in the Si band gap at the interface, corresponding to the charge neutrality level (E_{CNL}).¹ The energy difference (~ 0.20 eV) between E_{CNL} and E_F introduces charge transfer through the interface, generating intrinsic dipoles around the interface. It results in a valence band edge (VBE) at about -0.4 eV. This corresponds to SBH of 0.4 eV for a hole, being in a good agreement with the experiments.²¹

When a B atom is incorporated at the interface, VBE shifts due to charge transfer induced by a B atom. Figure 4(a) shows calculated LDOS at $z = 1.59$ nm using a (1×1) cell with a B atom doped at position c in Fig. 1(a) (upper panel) as well as that without a B atom (lower panel).

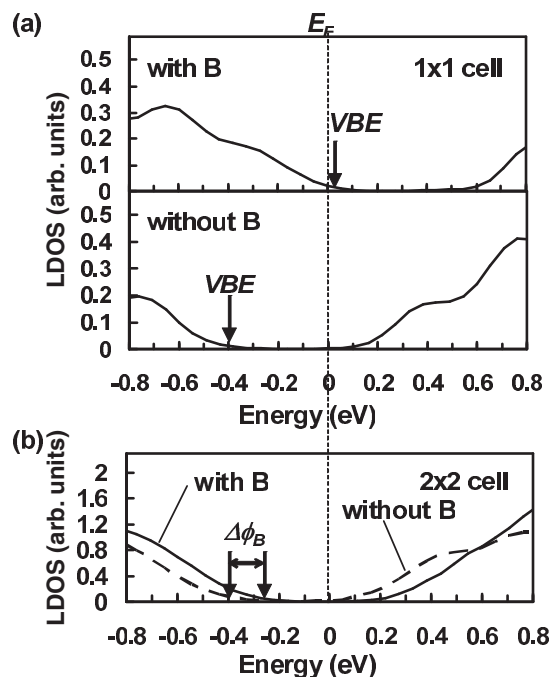


FIG. 4. (a) Calculated LDOS at 1.59 nm from the interface for a (1×1) unit cell with (upper) and without a B atom (lower). (b) Those calculated for a (2×2) unit cell at 1.59 nm from the interface in with (solid) and without a B atom (broken).

With a B atom, VBE moves beyond E_F hence the SBH would be zero or even negative. Then the SBH reduction width $\Delta\phi_B$ is larger than 0.45 eV, as shown in Fig. 4(a). This drastic SBH reduction arises from a large dipole between B and Si across the interface as discussed in Fig. 2.

We also performed the calculation with a (2×2) unit cell with and without B as shown in Fig. 4(b). A B-doped (2×2) unit cell has only one B atom at one of the positions corresponding to c in Fig. 1(a), meaning that B concentration is 4 times lower than the (1×1) cell. It should be noted that the position of VBE without B is the same as that for (1×1) , indicating that our calculation results do not contain errors owing to the cell size.

Figure 4(b) shows $\Delta\phi_B = 0.15$ eV, which is smaller than the (1×1) case. The difference of $\Delta\phi_B$ can be attributed to B concentration at the interface. A single B atom in (1×1) and (2×2) unit cells corresponds to 2.85×10^{21} and 7.13×10^{20} cm^{-3} , respectively.

III. EXPERIMENTAL VERIFICATION

A. Sample preparation

To verify our theoretical results, we experimentally analyzed B profiles and measured I - V characteristics of B-doped NiSi/Si diodes. We prepared NiSi/Si Schottky diodes through ion implantation after silicidation process.²² First, a Ni layer of 20-nm thickness was deposited on a Si substrate followed by the annealing process at 450°C Si substrate. The quality of the interface between NiSi and Si is atomically clean because it is defined by the frontier of Ni migration. B ions were implanted into the NiSi/Si diodes at 10 keV with the dose of 10^{15} cm^{-2} followed by drive-in annealing.

B. B profiles in the vicinity of the interface

Most of B atoms in the vicinity of NiSi/Si interface are in the interstices right after implantation. Since the formation energy of an interstitial B atom is the largest at the position **i** in Fig. 1(a), these B atoms migrate toward the interface and fall into substitutional sites during the subsequent annealing process, as illustrated by an arrow in Fig. 1(b).

On the Si side of the interface, the lower-energy valley of the formation energy appears owing to dipole formation, as discussed above. This energy valley can raise the solubility limit at the interface above that for the bulk Si. The solubility limit at the interface $C_{\text{sol}}^{\text{int}}$ can be expressed by

$$C_{\text{sol}}^{\text{int}} = C_{\text{sol}}^{\text{bulk}} \exp\left(-\frac{\Delta}{kT}\right), \quad (4)$$

where $C_{\text{sol}}^{\text{bulk}}$ (a function of T), Δ and T denote the solubility limit of B in the bulk Si, the depth of the valley and the annealing temperature, respectively.²³ Note that Δ is a function of $C_{\text{sol}}^{\text{int}}$ because of repulsive B-B interaction and hence Eq. (4) should be treated self-consistently. In fact, the obtained Δ 's for (1×1) unit cell [$\Delta^{(1 \times 1)}$] and for (2×2) unit cell [$\Delta^{(2 \times 2)}$] are -0.45 and -0.58 eV, respectively, showing that higher B concentration (i.e., stronger B-B interaction) results in smaller $|\Delta E|$.

Using Eq. (4) with the calculated results, we estimated $C_{\text{sol}}^{\text{int}}$. We assumed that Δ exponentially saturates toward Δ^{sat} as B-B distance d increases. Since the calculation of exact Δ^{sat} is difficult because of computational capacity, we presumed Δ^{sat} by extending the results of bulk formation energies. The difference between B formation energies in a bulk Si ($2 \times 2 \times 2$) and a well-saturated ($4 \times 4 \times 4$) cell is 0.06 eV.²⁴ We extended this difference to the junction structure and assumed $\Delta^{\text{sat}} = \Delta^{(2 \times 2)} - 0.06 = -0.64$ eV. Even though this assumption is rough and may contain an error more or less, this does not make big difference in the range of our discussion.

Connecting $\Delta^{(1 \times 1)}$, $\Delta^{(2 \times 2)}$, and Δ^{sat} exponentially as a function of d , we obtain a Δ - C curve, where $C = d^{-3}$ is the B concentration in a unit cell.

Another Δ - C curve is given by Eq. (4) at a certain temperature T , where $C_{\text{sol}}^{\text{bulk}}$ is obtained by fitting the experimental data taken from the literature.²⁵

The crossing point of these two curves gives $C_{\text{sol}}^{\text{int}}$ at the temperature T . The obtained $C_{\text{sol}}^{\text{int}}$ is plotted as a function of T in Fig. 5(a). It is predicted that $C_{\text{sol}}^{\text{int}}$ can exceed $C_{\text{sol}}^{\text{bulk}}$ by two or three orders, which will be verified experimentally below.

Figure 5(b) shows B profiles in the NiSi/Si diodes before and after the drive-in annealing process at 550° C for 30 seconds obtained by means of the atom-probe analysis. The profiles are taken along the direction perpendicular to the local surface of the interface defined as the isosurface where the atomic concentration of Ni is 25% (proximity diagram). Therefore broadness of the profile arising from the roughness of the interface is eliminated in these profiles. Whereas the B profile around the interface is almost flat in the unannealed case, a sharp peak whose full width at half maximum is about 1.5 nm appears after the annealing process. The summit is obtained at 0.15 nm from the interface on the Si side by fitting the peak with a polynomial, which agrees well with the position of **c** in Fig. 1(b). The maximum B concentration is

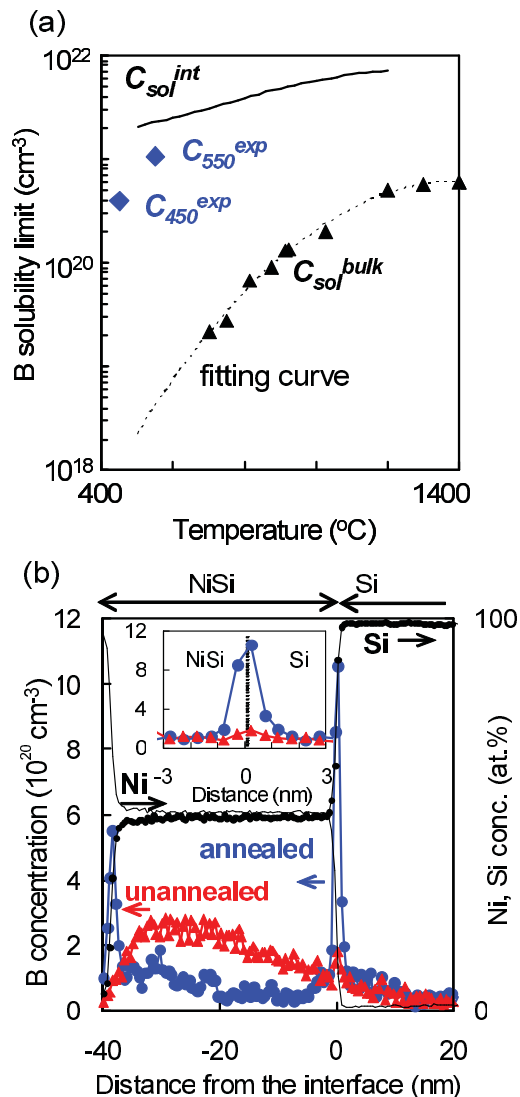


FIG. 5. (Color online) (a) Calculated solubility limit of B atoms at the interface of NiSi/Si ($C_{\text{sol}}^{\text{int}}$) is plotted together with that in the bulk Si ($C_{\text{sol}}^{\text{bulk}}$) taken from the literature²⁵ (filled triangles). Experimentally observed values C_{550}^{exp} and C_{450}^{exp} are plotted by diamonds. (b) B, Ni, and Si profiles in NiSi/Si diode samples fabricated through the ion-implantation after silicidation process obtained by atom-probe analysis. Blue and red symbols denote the B profiles in a sample annealed at 550° C and in an unannealed one, respectively. Inset: magnified profiles in the vicinity of the interface.

$C_{550}^{\text{exp}} = 1.1 \times 10^{21} \text{ cm}^{-3}$. We also analyzed a sample annealed at 450° C and obtained $C_{450}^{\text{exp}} = 4.0 \times 10^{20} \text{ cm}^{-3}$. As expected by theoretical results, both of these values far exceed the bulk solubility limit $C_{\text{sol}}^{\text{bulk}}$ as plotted in Fig. 5(a).

C. Measurement of SBH modulation

Although we observed a sharp and high B concentration peak, which is in good agreement with theoretical prediction, it is difficult to know whether or not these B atoms are actually at substitutional sites.

Therefore we measured the electrical characteristics of the B-incorporated NiSi/Si diode to extract the SBH value. If most

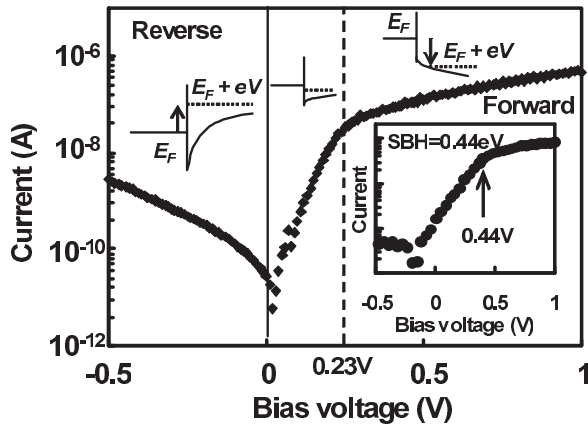


FIG. 6. I - V characteristics of NiSi/Si diode with B implantation followed by drive-in annealing at 450°C measured at 25 K. A shoulder structure of the forward current at 0.23 V indicates the SBH. Inset: a typical I - V characteristics of NiSi/ p^- -Si diode (without B implantation) whose SBH is 0.44 eV. A shoulder structure at 0.44 V corresponds to the SBH.

of the B atoms are not in the substitutional but in interstitial sites, SBH will not be reduced because interstitial B atoms do not cause charge transfer hence do not contribute to SBH modulation.

Figure 6 shows the I - V characteristics of a B-implanted NiSi/Si diode for which drive-in annealing was performed at 450°C . $C_{\text{sol}}^{\text{bulk}}$ at this temperature is lower than $2 \times 10^{18}\text{ cm}^{-3}$ as can be seen in Fig. 5 (a). The diode characteristics were measured at 25 K. At this low temperature we can eliminate the band-bending effect that leads to underestimation of the SBH, because most of the acceptors of $2 \times 10^{18}\text{ cm}^{-3}$ in the bulk Si are frozen out and the charge concentration is as low as $2 \times 10^{17}\text{ cm}^{-3}$.²⁶

The diode characteristics in Fig. 6 has a shoulder structure; the forward current sharply decreases under 0.23 V. This indicates that the carrier transport is strongly suppressed by the Schottky barrier under this voltage. In fact, a typical diode characteristic of NiSi/ p^- -Si whose SBH is 0.44 eV (Ref. 12) has a shoulder structure at around 0.44 V as shown in the inset. Therefore we can estimate the SBH of this diode to be 0.23 eV, and $\Delta\phi_B$ is about 0.2 eV.

This large $\Delta\phi_B$ can be attributed to dipoles induced by B atoms in the Si substitutional sites at the interface as theoretically predicted; it cannot be explained by the band-bending effect because the charge concentration is quite low at the measurement temperature as explained above.

Comparing with theoretical predictions of $\Delta\phi_B = 0.15\text{ eV}$ for $7.13 \times 10^{20}\text{ cm}^{-3}$, our experimental $\Delta\phi_B = 0.2\text{ eV}$ with

the B concentration of $4.0 \times 10^{20}\text{ cm}^{-3}$ is quite consistent to presume that most of the B atoms at the interface are in the substitutional sites.

IV. DISCUSSION

It has been shown that dipoles induced by B atoms at the interface of NiSi/Si have drastic effects on the B solubility limit and SBH. One question arising from our results is whether further modulation of SBH is possible.

Elements of group II such as magnesium (Mg) or beryllium (Be) are candidates for a larger SBH reduction, because they are expected to be more negatively charged than group III elements including B and hence generate larger dipoles across the interface.²² To investigate whether or not those impurities actually migrate into Si substitutional sites at the interface to generate large dipoles, we need to discuss the dynamics as well as the formation energies.

Our discussion in this paper is based on the formation energies only, and dynamics including energy barriers is not considered. We believe this approach is valid in the case of B in Si, because the migration energy of an interstitial B atom in Si is so small as compared to the formation energy,²⁷ and hence we do not need to consider the dynamics. On the other hand, since the diffusion mechanisms of Mg or Be are not clear at this moment we have no guarantee that our discussion of B can be extended.

Therefore, the potential of Mg and Be for further SBH modulation should be discussed not only based on formation energies but also on their diffusion dynamics in Si and metal/Si interface. This work will be done in the near future.

V. CONCLUSION

In conclusion, we have theoretically shown that a B atom placed at the interface of NiSi/Si is energetically stable due to dipole generation across the interface, and this dipole induces a large SBH modulation and a remarkable increase in the solubility limit of the dopant around the interface. These theoretical results were confirmed by experimental analysis of the B-implanted NiSi/Si Schottky diodes.

ACKNOWLEDGMENTS

The authors thank N. Aoki, K. Ohuchi, K. Suguro, H. Akutsu, A. Hokazono, S. Kawanaka, Y. Nakazaki, T. Shimizu (Toshiba Corporation), and J. Yamauchi (Keio University) for fruitful discussions.

¹J. Tersoff, *Phys. Rev. Lett.* **52**, 465 (1984).

²S. G. Louie, J. R. Chelikowsky, and M. L. Cohen, *Phys. Rev. B* **15**, 2154 (1977).

³W. Mönch, *Appl. Phys. Lett.* **72**, 1899 (1998).

⁴H. Hasegawa and H. Ohno, *J. Vac. Sci. Technol. B* **17**, 1867 (1999).

⁵W. E. Spicer, I. Lindau, P. Skeath, C. Y. Su, and Patrick Chye, *Phys. Rev. Lett.* **44**, 420 (1980).

⁶R. T. Tung, *Phys. Rev. Lett.* **52**, 461 (1984).

⁷H. Fujitani and S. Asano, *Phys. Rev. B* **42**, 1696 (1990).

- ⁸R. T. Tung, *Phys. Rev. Lett.* **84**, 6078 (2000).
- ⁹R. A. McKee, F. J. Walker, M. Buongiorno Nardelli, W. A. Shelton, and G. M. Stocks, *Science* **300**, 1726 (2003).
- ¹⁰C. Berthod, N. Binggeli, and A. Baldereschi, *Phys. Rev. B* **68**, 085323 (2003).
- ¹¹V. De Renzi, R. Rousseau, D. Marchetto, R. Biagi, S. Scandolo, and U. del Pennino, *Phys. Rev. Lett.* **95**, 046804 (2005).
- ¹²S. P. Murarka, *Silicides for VLSI Applications* (Academic Press, London, 1983).
- ¹³K. Kato, T. Uda, and K. Terakura, *Phys. Rev. Lett.* **80**, 2000 (1998).
- ¹⁴D. Vanderbilt, *Phys. Rev. B* **41**, 7892 (1990).
- ¹⁵K. Kato, D. Matsushita, K. Muraoka, and Y. Nakasaki, *Phys. Rev. B* **78**, 085321 (2008).
- ¹⁶W. B. Pearson, *Handbook of Lattice Spacing and Structures of Metals and Alloys* (Pergamon, New York, 1958).
- ¹⁷R. M. Boulet, A. E. Dunsworth, J.-P. Jan, and H. L. Skriver, *J. Phys. F* **10**, 2197 (1980).
- ¹⁸M. Tsuchiaki, K. Ohuchi, and A. Nishiyama, *Jpn. J. Appl. Phys.* **44**, 1673 (2005).
- ¹⁹F. F. Zhao, Y. P. Feng, Y. F. Dong, and J. Z. Zheng, *Phys. Rev. B* **74**, 033301 (2006).
- ²⁰H. Wu, P. Kratzer, and M. Scheffler, *Phys. Rev. B* **72**, 144425 (2005).
- ²¹E. Bucher, S. Schulz, M. Ch.Lux-Steiner, and P. Munz, *Appl. Phys. A* **40**, 71 (1986).
- ²²T. Yamauchi, Y. Nishi, Y. Tsuchiya, A. Kinoshita, J. Koga, and K. Kato, IEDM Tech. Dig., 963 (2007).
- ²³Chris G. Van de Walle, D. B. Laks, G. F. Neumark, and S. T. Pantelides, *Phys. Rev. B* **47**, 9425 (1993).
- ²⁴J. Yamauchi (private communication).
- ²⁵G. L. Vick and K. M. Whittle, *J. Electrochem. Soc.* **116**, 1142 (1969).
- ²⁶F. J. Morin and J. P. Maito, *Phys. Rev.* **96**, 28 (1954).
- ²⁷C. S. Nichols, C. G. Van de Walle, and S. T. Pantelides, *Phys. Rev. B* **40**, 5484 (1989).